Technical Report

Mechanical and Corrosion Performance of CRA OCTG After Long Time Exposure in Corrosive Environments in Actual Field Service

Yusaku TOMIO*
Hisashi AMAYA
Masaki UEYAMA
Masayuki SAGARA
Takashi DOI
Yuhei SUZUKI

Abstract

Corrosion resistant alloys (CRAs) have been used in exploration and production fields with harsh environments. In this study, a surface film on the Ni based alloy (UNS N08535) was analyzed and compared with that formed after corrosion testing in a laboratory. The surface film structure after exposure in the actual well was composed of sulfides and oxides and this thin layer structure is consistent with laboratory results using small-scale specimens during a short exposure time. These results demonstrate the effectiveness of the proposed corrosion resistant mechanism against corrosive environments.

1. Introduction

The demand for primary energy has been increasing significantly with the increase in population and modernization. Although oil consumption is predicted to decrease in the present environment, where CO_2 emissions must be reduced sharply, the demand for natural gas is expected to increase as it replaces coal and oil. As of 2023, with the addition of purchasing restrictions on Russian-produced natural gas due to Russia's invasion of Ukraine, natural gas development has been progressing steadily, as has drilling in high-temperature and high-pressure environments with high concentrations of hydrogen sulfide.

Corrosion resistant alloys (CRAs) are required for drilling of high-temperature and high-pressure natural gas reservoirs where CO_2 and hydrogen sulfide concentrations are high and where the formation water contains a fairly large amount of chloride ion. The CRAs have been used as oil country tubular goods (OCTGs) for high-temperature and high-pressure environments, utilizing their characteristic corrosion resistance and strength.[1–6] The CRAs have high concentrations of Cr, Ni, and Mo, so corrosion-resistant film is formed even in the harsh environments mentioned above.

In many offshore natural gas wells that may become corrosive environments, well design has been performed using CRAs as OCTG pipes. This is because the use of CRAs ensures the lowest life cycle cost and allows operators to continue production without suspensions for workovers caused by the corrosion of OCTG materials, etc. Austenitic alloys and Ni-based alloys that have high Ni and Mo contents are specified as Group 3 and Group 4, respectively, in the international oil and natural gas standard API 5CRA/ISO 13680.[7] They have been commonly used in environments that have high temperature and produce hydrogen sulfide simultaneously. By increasing Ni and Mo concentrations, these alloys form stable surface passive film that protects their interior from corrosion. However, the formation and stability of the film on the surfaces of CRAs in corrosive environments have only been evaluated by laboratory tests. In addition, the durations of these tests were mostly from 2 weeks to 3 months, and very few tests lasted 6 months or more. There have been almost no reports on whether this passive film remains stable after exposure to actual well environments. Furthermore, few studies have investigated whether the tensile strength, hardness, and other mechanical properties of CRAs would change over long-term use in high-temperature and high-pressure environments. To answer the above question, the present study has also examined whether these mechanical properties would be affected by long-term exposure to an actual corrosive environment.

Figure 1 shows the chart Nippon Steel Corporation uses to select OCTG materials for specific well environments.[8] For environments where the CO_2 partial pressure is 0.02 MPa or higher and CRAs are required, the primary decision on material selection is

* Ph.D, Senior Researcher, Steel Products Research Dept., Kansai R & D Lab.
1850 Minato, Wakayama City, Wakayama Pref. 640-8555

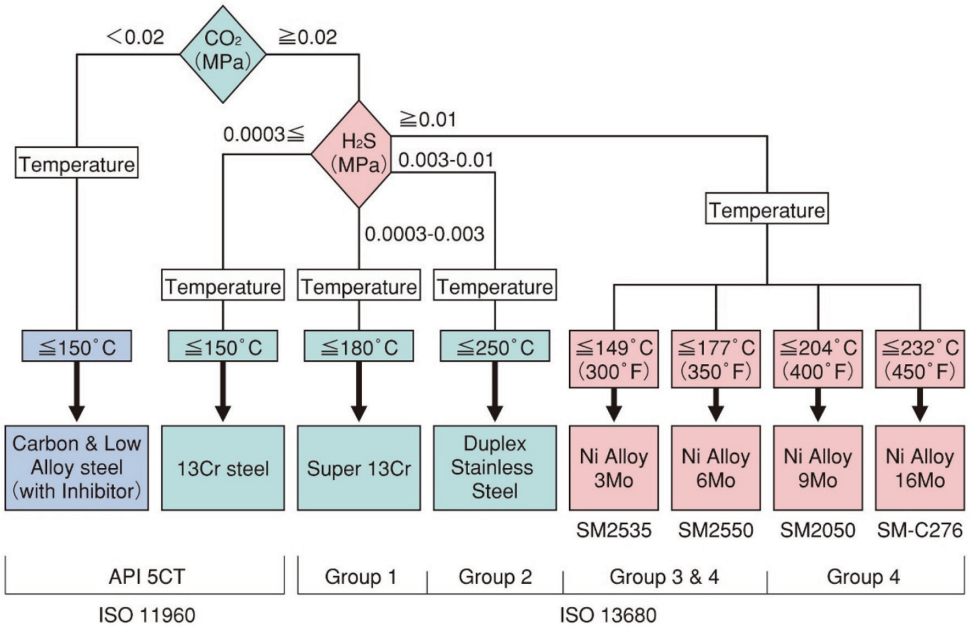

Fig. 1 Material selection chart for oil and gas development

Table 1 An actual environmental well condition in the Middle East

Bottom hole pressure	31 MPa
Bottom hole temperature	104°C (220°F)
H_2S	1 mol% in gas (0.31 MPa)
CO_2	3 mol% in gas (0.69 MPa)
Water	Only condensed water
Elemental sulfur	None

made based on two factors: the H_2S partial pressure and the maximum operating temperature. This selection needs to be evaluated more rigorously and appropriate materials are finally selected according to the required strength of the material under the mechanical load predicted from the well design, the expected pH of the exposed environment, the chloride ion concentration in the formation water, etc. **Table 1** shows the environmental conditions of a natural gas reservoir in the Middle East. For this environment, UNS N08535 shown as "Ni Alloy 3Mo" in Fig. 1 with a specified minimum yield strength of 758 MPa was selected. The tubings were manufactured at Nippon Steel and used as an actual production tubing continuously exposed to production fluids in the well. After 15 years of production, the well was worked over. The workover was carried out for reasons different from the integrity of the material. Since CRAs are typically intended to be maintenance-free, there is little opportunity to analyze these tubing products exposed to corrosive environments for long periods. In this study, we investigated the mechanical properties of this UNS N08535 tubing used in the actual environment for a long time and compared them with those of new UNS N08535 tubing. We also investigated the corrosion resistant film formed on the inner surface of the used tubing and compared it with that formed in laboratory corrosion tests.

2. Experimental Methods

We investigated the mechanical properties, microstructures, surface corrosion state, and passive film on the inner surface of the UNS N08535 pipes used in the actual environment (hereafter referred to as the field-experienced pipes). The evaluation was conducted by comparing the pipes exposed to the actual production environment with pipes manufactured at the same time but stored without being used (hereafter referred to as the unused pipes). The test specimen for microstructure observation was machined in a direction longitudinal to the rolling direction of the pipe. The specimen for cross-sectional observation was mechanically polished with SiC paper and then polished with alumina slurry. After chemical etching by submerged swabbing with a solution of Etchant 94 in ASTM E407, the microstructure was observed by an optical microscope at 100X and 400X magnifications.

Tensile tests were conducted according to API 5CRA first edition (third edition of ISO 13680). High-temperature tensile tests were conducted at 50, 100, 150, and 200°C according to ASTM E21-09. Charpy impact tests evaluated the toughness of the field-experienced and unused pipes. Due to the limitation of the pipe wall thickness (about 9 mm), sub-size specimens (10 mm × 5 mm) were used. The specimens were taken in a direction transversal to the rolling direction of the pipe, and the notch direction was longitudinal.

The slow strain rate test (SSRT) was conducted in accordance with NACE TM0198-2011[9] to evaluate the susceptibility of the pipes to stress corrosion cracking (SCC). Uniaxial tensile specimens 3.81 mm in diameter and 25.4 mm in gauge length were used in the SSRT. The evaluation environment was a solution containing 25% NaCl and 0.5% CH_3COOH by weight under 0.7 MPa H_2S at 149°C. The strain rate was $4 \times 10^{-6} s^{-1}$. Both field-experienced and unused pipes were evaluated in both inert and corrosive environments. The test results were evaluated by comparing the reduction in area and the total time to fracture in the corrosive environment with those in the inert environment. Three specimens were taken from the unused pipes and evaluated. For the field-experienced pipe, the bottom portion (B-1), middle portion (B-2), and top portion (B-3) were evaluated.

Auger electron spectroscopy (AES) was conducted on both the used and unused pipes to investigate the properties of the film

formed on their surfaces. The specimens were rinsed in deionized water and degreased with acetone. AES was performed on a region of about 10 nm in diameter at a prior beam voltage of 10 kV. Element concentration profiles in the depth direction were obtained by sputtering the surface with Ar^+ ions. The sputtering speed was 0.9 nm/min as SiO_2 conversion.

3. Results and Discussion

3.1 Appearance

The outer surfaces of the unused and field-experienced pipes are shown in **Figs. 2** (a) and (b), respectively. Their inner surfaces after cutting are shown in Figs. 2 (c) and (d), respectively. Almost no surface flaws were found, and no obvious traces of corrosion or cracks were observed. Compared to the shiny metallic surface of the unused pipe, the inner surface of the field-experienced pipe was somewhat dull. This difference in the surface condition was thought to arise from the difference in the structure of the surface film. No major differences were observed in the outer surfaces of both pipes. Therefore, the production fluid was considered to have affected the structure of the surface film and caused the color difference on the inner surface.

3.2 Microstructures and mechanical properties

Figures 3 (a) and (b) show the longitudinal cross-sectional microstructures of the unused and field-experienced pipes near the outer and inner surfaces, respectively. These microstructures are typical of cold-worked austenitic alloys. The strain introduced by cold working is clearly visible. The grain size was uniform in both the

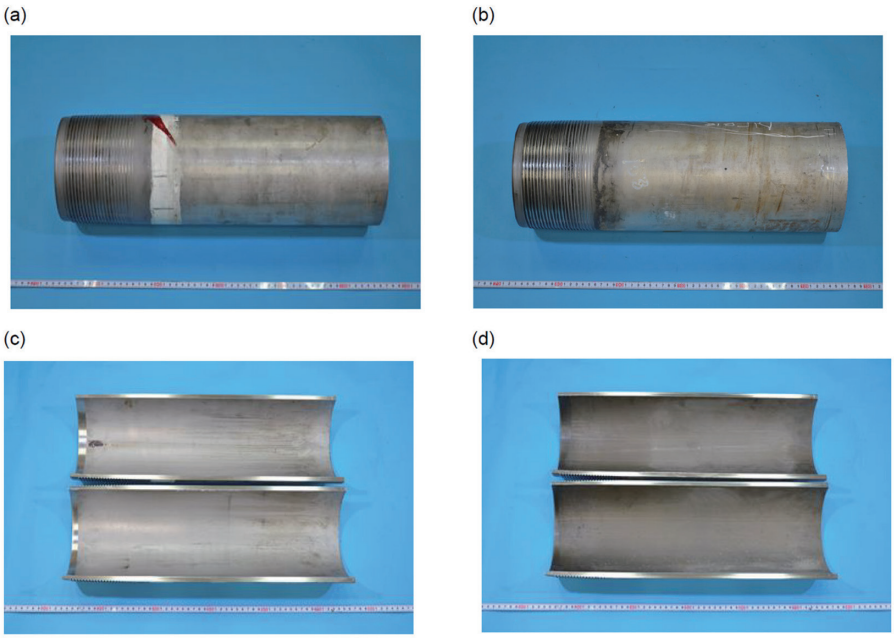

Fig. 2 Appearances of the pipes; (a) outer surface of unused pipe, (b) outer surface of field-experienced pipe, (c) inner surface of unused pipe, and (d) inner surface of field-experienced pipe

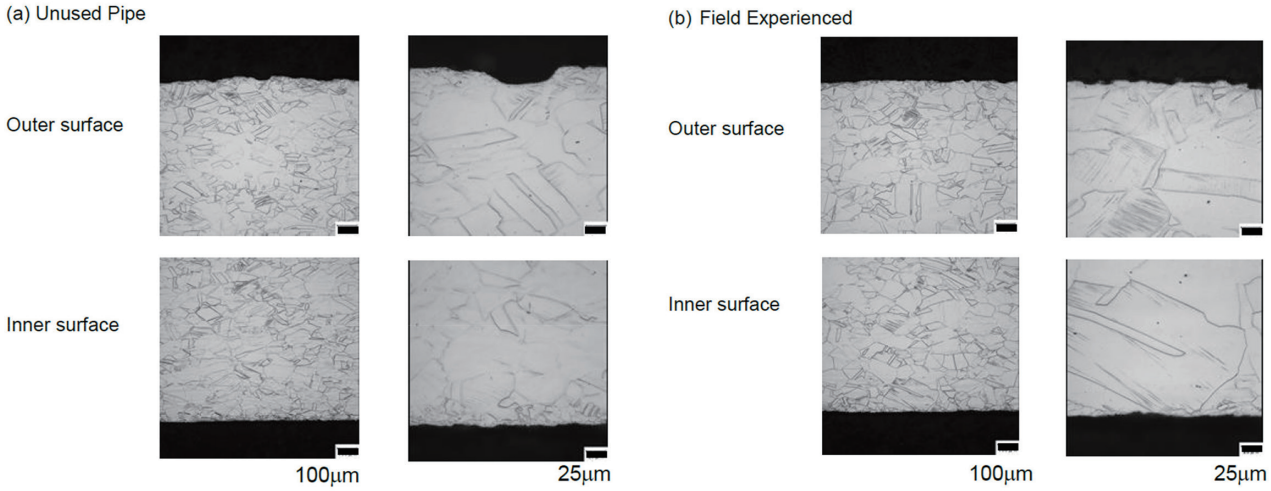

Fig. 3 Microstructure of pipes; (a) the unused pipe and (b) the field-experienced pipe

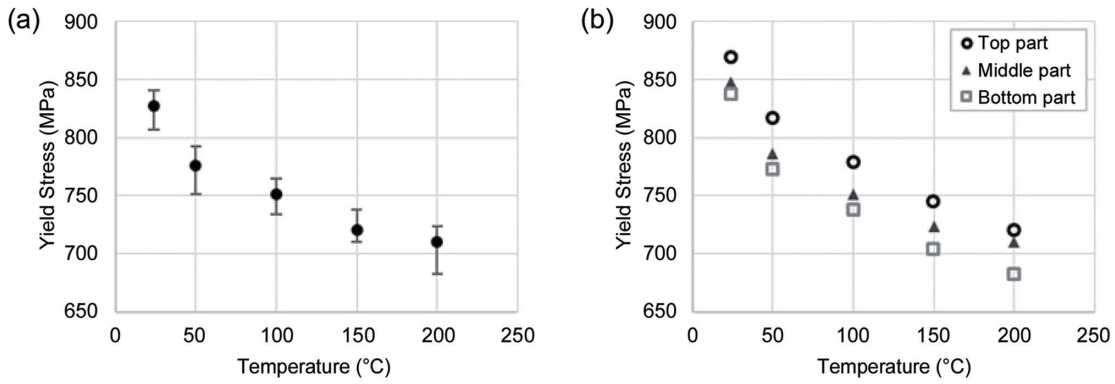

Fig. 4 Yield stress of the pipes at room and elevated temperatures; (a) the unused pipe and (b) the field-experienced pipe

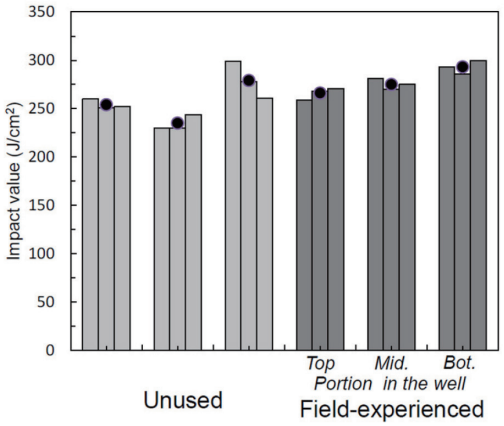

Fig. 5 Impact values of the pipes evaluated by Charpy impact test at −10°C (individual values and the averaged value are indicated by bars and dots, respectively)

unused and field-experienced pipes. Precipitates and intermetallic compounds were not observed either inside the grains or on the grain boundaries. **Figures 4** (a) and (b) show the results of tensile tests conducted at room and elevated temperatures on the unused and field-experienced pipes, respectively. The unused pipe was tested three times, while the field-experienced pipe was tested in the positions corresponding to the top, middle, and bottom portions of the well. The average, minimum, and maximum values of the yield stress are also shown in Fig. 4. The results indicate that the field-experienced pipe achieved a minimum yield stress of 758 MPa at 25°C as the unused pipe did. **Figure 5** shows the results of the Charpy impact test conducted on the unused and field-experienced pipes. There was no significant difference in impact values between the unused and field-experienced pipes. No aging effect was confirmed in the well environment.

Compared to the unused pipes, the field-experienced pipes showed that their mechanical properties were not affected by 15 years of exposure to the well environment. These results confirmed the stable performance of UNS N08535 as a CRA material during long-term use.

3.3 Stress corrosion cracking (SCC) resistance

An SSRT test was conducted to evaluate the SCC susceptibility of both the field-experienced and unused pipes. **Table 2** compares the time to fracture and reduction in area of the unused pipes in the corrosive environment simulating the well environment and those in the inert environment. All specimens exceeded the specified threshold values. This confirmed that they exhibited sufficient SCC resistance in the corrosive environment. **Table 3** shows the SSRT results of the field-experienced pipes. The SSRT results of specimens taken from the top, middle, and bottom of the well showed that the total time to fracture (TTF) ratio and reduction in area (RA) ratio of all specimens exceeded 0.90, confirming sufficient SCC resistance. From the above results, it was concluded that the corrosion resistance of the field-experienced pipes was not different from that of the unused pipes.

Table 2 SSRT results of the unused pipe under sour condition

Item	Environment	TTF (hours)	RA (%)	TTF ratio	RA ratio	Remark
A-1	Inert	7.96	77.55	-	-	-
	Hostile	8.09	72.86	1.02	0.94	No SCC
A-2	Inert	7.53	71.91	-	-	-
	Hostile	7.64	71.63	1.01	1.00	No SCC
A-3	Inert	7.88	77.55	-	-	-
	Hostile	8.02	70.51	1.02	0.91	No SCC
Criteria	-	Min. 6	Min. 25	Min. 0.80	Min. 0.80	No SCC

Table 3 SSRT results of the field-experienced pipe under sour condition

Item	Environment	TTF (hours)	RA (%)	TTF ratio	RA ratio	Remark
B-1	Inert	8.46	77.80	-	-	-
	Hostile	8.62	72.73	1.02	0.93	No SCC
B-2	Inert	9.56	81.21	-	-	-
	Hostile	9.55	75.91	1.00	0.93	No SCC
B-3	Inert	9.76	79.36	-	-	-
	Hostile	9.60	71.35	0.98	0.90	No SCC
Criteria	-	Min. 6	Min. 25	Min. 0.80	Min. 0.80	No SCC

3.4 Results of surface analysis after long-term exposure

The corrosion resistance of CRAs is achieved by alloying elements that form a surface film inhibiting anodic dissolution in the environment. **Figure 6** shows the inner surface appearances and

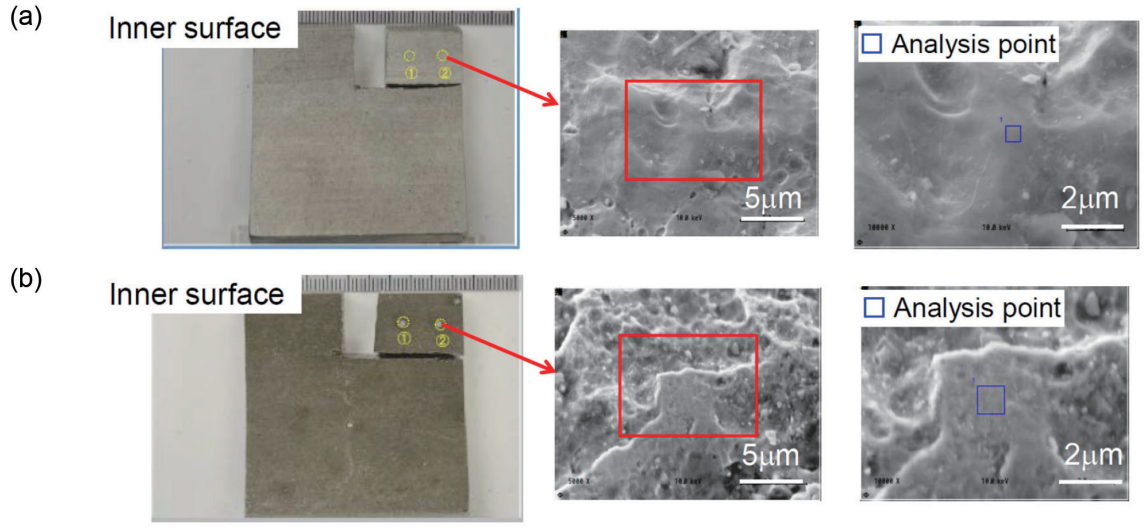

Fig. 6 Appearance of inner surface, SEM images of the correspoding site, and analysis point of AES; (a) unused pipe and (b) field-experienced pipe

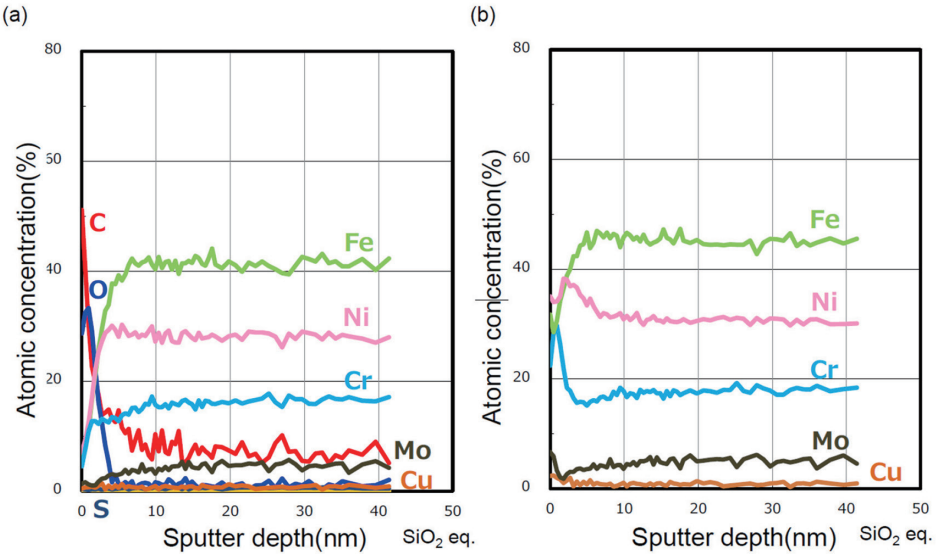

Fig. 7 AES depth profile of inner surface of unused pipe; (a) profiles of all elements and (b) normalized profile for metallic elements after removing C, O, S

SEM images of the AES analysis points of the unused and field-experienced pipes. **Figure 7** shows the AES concentration profiles of elements on the inner surface of the unused pipe. The concentration profiles of all elements are shown in Fig. 7(a), while the normalized profiles of the metal elements by excluding the concentrations of oxygen (O), carbon (C), and sulfur (S), are shown in Fig. 7(b). The concentration profiles of all elements suggest that O is enriched in the outermost surface of the film. The O-enriched layer is roughly 2 to 3 nm in thickness and is considered to be an oxide layer. The enrichment of C is also observed, but this is thought to be ascribed to the contamination of the specimen. In the concentration profiles of only the metal elements, the enrichment of Cr and Mo near the surface corresponds to the peak position of O, suggesting the formation of Cr and Mo oxides. Even in the unused pipes, Cr is enriched in the oxide film, but no sulfide film was observed to be formed by exposure to an environment containing hydrogen sulfide. **Figure 8** shows the AES profiles of elements in the inner surface of the field-experienced pipe. In the concentration profiles of all elements in Fig. 8(a), S is significantly enriched in the surface, and the enrichment of O is observed underneath. The thickness of the S-enriched layer was about 10 nm, and the O-enriched layer was about several tens of nanometers thick. The enrichment of C near the surface is thought to have been derived from the contamination of the specimen, as noted for the unused pipe. Figure 8(b) shows the normalized concentration profiles of the metal elements by excluding C, O, and S. The region where Ni, Mo, and Cu show high concentration corresponds to the regions where S is enriched. The profile of Cr corresponds to that of O, and Cr was present under the sulfide film.

In addition to AES, the surface film of the field-experienced pipe was cross-sectionally observed by transmission electron microscopy (TEM) equipped with an energy dispersive X-ray spectrometer (EDS). **Figure 9** shows a cross-sectional TEM micrograph of the outermost surface. It can be seen that a surface film exists between the bulk and the resin used for embedding the specimen. The thick-

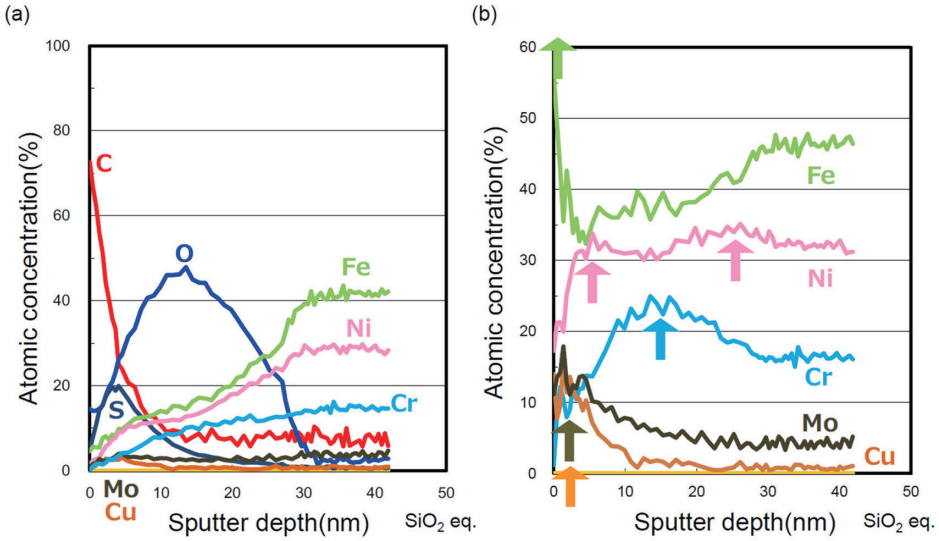

Fig. 8 AES depth profile of inner surface of field-experienced pipe; (a) profiles of all elements and (b) normalized profile for metallic elements after removing C, O, S

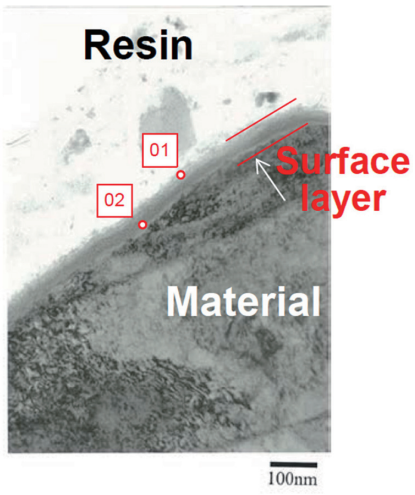

Fig. 9 Transmission electron microscope image at the inner surface of field-experienced pipe

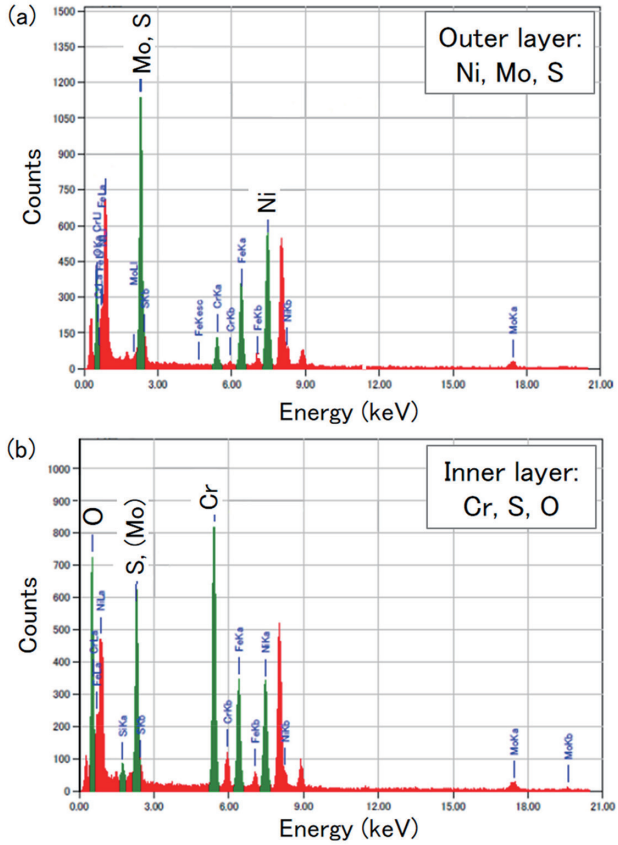

Fig. 10 Energy dispersive X-ray spectrum and identified elements; (a) point 01 and (b) point 02

ness of the surface layer was measured to be several tens of nanometers. This value matched the thickness observed by AES. The element concentrations in the surface film layer were measured at the two points 01 and 02 shown in Fig. 9, using the EDS. The enrichment of S is observed along with Ni and Mo at the point 01 in the layer on the outer surface side as shown in **Fig. 10**(a). Cr, O, and S were detected at the point 02 in the layer as shown in Fig. 10(b). The results agreed well with the AES observation results that Ni and S, and Cr and O were observed at the same positions, respectively. This direct observation of the surface film revealed that the surface film on the field-experienced pipe consists of the outermost Ni sulfide and Cr oxide formed underneath. In the following discussion, we compared the surface film formed in the actual environment with the film formed in a simulated laboratory test environment. A previous laboratory study found that the surface film formed on a 25%Cr-32%Ni-3%Mo alloy in a hydrogen sulfide-containing environment at 149°C consisted of an outer layer of Ni sulfide and an inner layer of Cr oxide.[10] On the other hand, the present study showed that the film structure after long-term exposure to the actual well environment also consists of Ni sulfide and Cr oxide. The structure of this surface film agreed with that formed on the surface of small-size specimens in a relatively short-term corrosion test in a laboratory.

These results confirm that the corrosion resistance mechanism of Ni-based alloys in a hydrogen sulfide-containing environment, as proposed through basic research, is also effective in the actual well environment containing hydrogen sulfide. The effectiveness of material selection for specific environments based on the corrosion resistance mechanism was also verified. For future research, it will be necessary to investigate how the formation of the surface film is affected by environmental conditions different from those in the present study, with particular focus on temperature and partial pressure of hydrogen sulfide.

4. Conclusions

- The mechanical properties and corrosion resistance of the corrosion-resistant alloy UNS N08535 did not change even after long-term exposure to an actual well environment.
- The structure of the surface film after exposure to the actual well environment consists of the outermost Ni sulfide and underlying Cr oxide and is similar to that formed on laboratory specimens after short-time immersion.
- These results demonstrate the effectiveness of research on the mechanism of corrosion resistance in a laboratory-level corrosive environment containing hydrogen sulfide and also verify the validity of our material selection.

References

1) Kolts, J.: Laboratory evaluation of corrosion resistant alloys for the oil and gas industries, Corrosion/86, Paper No. 323, NACE, Houston, Texas, 1986
2) Chaung, H. E., Watkins, M., Vaughn, G. A.: Stress-corrosion cracking resistance of stainless alloys in sour environments, Corrosion/85, Paper No. 227, NACE, Houston, Texas, 1985
3) Rhodes, P. R.: Stress cracking risk in corrosive oil and gas wells, Corrosion/86, Paper No. 322, NACE, Houston, Texas, 1986
4) Ikeda, A., Igarashi, M., Ueda, M., Okada, Y., Tsuge, H.: Corrosion. 45, 838 (1989)
5) Ueda, M., Kudo, T.: Evaluation of SCC Resistance of CRAs in Sour Service, Corrosion/91, Paper No. 2, NACE, Houston, Texas, 1991
6) Ueda, M., Amaya, H., Okamoto, H.: Economical Nickel Base Alloy for Sour Environment at Elevated Temperature, Corrosion/97, Paper No. 25, NACE, Houston, Texas, 1997
7) ISO 13680:2010, Petroleum and natural gas industries—Corrosion-resistant alloy seamless tubes for use as casing, tubing and coupling stock—Technical delivery conditions
8) Ueda, M., Takabe, H.: Localized Corrosion Resistance of Ni Base Alloy in Sour Environments, 10th Middle East Corrosion Conf., held March 7–10 (Bahrain: NACE West Asian and African Region, Saudi Arabian Section, 2004)
9) NACE Standard TM0198-2011, Standard Test Method—Slow Strain Rate Test Method for Screening Corrosion-Resistant Alloys (CRAs) for Stress Corrosion Cracking in Sour Oilfield Service, NACE International, 2011
10) Sagara, M., Otome, Y., Amaya, H., Kimura, S., Igarashi, M., Ueda, M.: Development of High-strength Ni Alloy OCTG Material for Sour Environment, Corrosion /2011, Paper No. 11109, NACE, Houston, TX, 2011

Yusaku TOMIO
Ph.D, Senior Researcher
Steel Products Research Dept.
Kansai R & D Lab.
1850 Minato, Wakayama City, Wakayama Pref.
640-8555

Masayuki SAGARA
Dr. Eng.
Formerly Senior Researcher, Kansai R & D Lab.
Manager, Products development Div.,
Nippon Steel Stainless Steel Corporation

Hisashi AMAYA
Dr. Eng.
General Manager, Tubular Products Technology Div.,
Pipe & Tube Unit
Principal Researcher, Kansai R & D Lab.

Takashi DOI
Ph.D, Senior Researcher
Materials Characterization Research Lab.
Advanced Technology Research Laboratories

Masaki UEYAMA
Senior Manager
Tubular Products Technical Service & Solution Dept.
Tubular Products Technology Div.
Pipe & Tube Unit

Yuhei SUZUKI
General Manager
NIPPON STEEL EUROPE GmbH